Numerical Simulation of Nonequilibrium Plasma in an MHD Power Generator

Y. Yoshikawa* and S. Kabashima†
Tokyo Institute of Technology, Yokohama, Japan

r-θ two-dimensional, time-dependent simulations of nonequilibrium plasma are carried out to develop a stable plasma with a fully ionized seed in a disk-type closed-cycle MHD power generation system. The working gases were Ar/K, Ar/Cs, He/K, and He/Cs. For all of the working gases considered, stable plasma with a fully ionized seed is obtained in nearly the entire generator, except in the relaxation region close to the anode. As the seed material, cesium produces better performance than potassium. Even when helium is used as the working gas instead of argon, it is expected that good performance can be obtained by suitably adjusting the gas conditions, magnetic field, and load resistance.

Nomenclature

A	= energy loss due to collision
B	= $(0,0,B)$ magnetic field vector
e	= electon charge
E	= $(E_r,E_\theta,0)$ electric field vector
h	= Planck's constant; also channel height
j	= $(j_r,j_\theta,0)$ current density vector
k	= Boltzman constant
k_{fN}	= ionizatiuon rate for argon or helium
k_{fS}	= ionization rate of potassium or cesium
k_{rN}	= recombination rate of argon or helium
k_{rS}	= recombination rate of potassium or cesium
m_e	= mass of electron
m_i	= mass of ith particle
n_e	= electron number density
n_i^+	= number density of ith atom
n_i	= number density of ith ion
p_e	= electron pressure ($=n_ekT_e$)
Q_r	= radiative energy loss
S	= plasma surface
T_e	= electron temperature
T_g	= gas temperature
T_W	= wall temperature
t	= time
u	= $(u_r,0,0)$ heavy species flow velocity vector
u_e	= electron drift velocity
β	= Hall parameter
ϵ_i	= (ionization potential of ith atom)/k
ν_{e-i}	= collision frequency between electron and ith particle
σ	= electrical conductivity (σ_{ideal})

Subscripts

i	= particle
N	= noble gas atom (argon or helium)
r,θ	= coordinate direction
S	= seed atom (potassium or cesium)

Received Dec. 20, 1985; revision received May 9, 1986.

*Graduate Student, Department of Energy Sciences.
†Associate Professor, Department of Energy Sciences.

Introduction

IN a closed-cycle MHD power generation system using nonequilibrium plasma, the reduction of power caused by ionization instability can be eliminated by introducing the concept of a fully ionized seed.[1] Shock tunnel experiments and steady-state analyses performed by a group at the Tokyo Institute of Technology have confirmed the validity of this concept, especially in a disk generator.[2,3] Also, the dynamical realization of the fully ionized seed state has been studied and it supports the achievement of better power generation with stable plasma having a fully ionized seed.[4]

In our experiments and numerical analyses, argon is treated as the mother gas; however, the most efficient power generation is expected to be achieved with a plasma of helium gas. The steady-state analyses of a full-scale generator with helium gas shows high efficiency in a compact generator.[5] A high-enthalpy extraction experiment have been successfully performed in a shock tunnel facility.[6] Therefore, it is important to investigate the dynamical behavior of the plasmas of other working gases as well as of argon seeded with potassium. In the present study, the realization of a stable plasma with a fully ionized seed has been numerically simulated for several working gases, such as Ar/K, Ar/Cs, He/K, and He/Cs. We have examined how the magnetic field and load resistance, which control the Joule heating of the electron, affect the plasma of Ar/K; some of the dynamical properties of this are known from previous investigations.[4]

The plasma structure of working gas Ar/Cs is compared to that of Ar/K. Suitable working gas conditions to obtain a stable plasma are found with helium as the mother gas. In all cases, we can expect good generator performance in producing power.

Basic Equations and Numerical Model

The calculation is based on the two-temperature model equations of the closed-cycle MHD plasma.[7,8] The model equations of the MHD plasma used in this work are the same as those in Refs. 4 and 9. The plasma equations are given as

$$\frac{\partial n_e}{\partial t}+\nabla\cdot(n_e u_e)=\dot{n}_e \tag{1}$$

$$j+\frac{\beta}{B}j\times B=\sigma\left(E^*+\frac{1}{en_e}\nabla P_e\right) \tag{2}$$

$$\frac{\partial U_e}{\partial t}+\nabla\cdot(U_e u_e)=\frac{j^2}{\sigma}-A-p_e\nabla\cdot u_e-Q_r \tag{3}$$

Table 1 Values of the generator conditions used in the numerical calculations

Inert gas	Seed	Stagnant pressure, atm	Stagnant temperature, K	Seed fraction, $\times 10^{-5}$	Mach number	Magnetic field strength, T	Load resistance, Ω
Ar	K	6	2000	5	1.7	3.5	0.5, 0.78, 1.0
Ar	K	6	2000	5	1.7	2.5	0.5, 0.78, 1.0
Ar	Cs	6	2000	5	1.7	3.5	0.5, 0.78, 1.0
He	K	4	2000	7.5	1.7	3.5	0.6, 1.0
He	Cs	4	2000	7.5	1.7	3.5	0.6, 1.0

where

$$E^* = E + u \times B \qquad \dot{n}_e = \dot{n}_N + \dot{n}_S$$

$$U_e = (3/2)n_e kT_e + \epsilon_N n_N^+ + \epsilon_S n_S^+$$

N represents argon or helium gas, S potassium or cesium, and

$$\dot{n}_i = k_{fi} n_e n_i - k_{ri} n_e^2 n_i^+$$

where i denotes argon, helium, potassium, or cesium particles. The numerical values of the generation and recombination constants, ionization potential, and degree of degeneracy are the same as those in Ref. 10. A denotes the collision loss of the electrons and is given as

$$A = 3kn_e(T_e - T_g)\sum_i \frac{m_e}{m_i}\nu_{e-i}$$

where ions of argon, helium, potassium, or cesium atoms are taken as the ith particle. The radiative loss Q_r is introduced in Ref. 11.

In this numerical model, a cylindrical coordinate system (r, θ) is used to specify the disk geometry and the magnetic field is considered to be perpendicular to the disk plane. Charge neutrality and low magnetic Reynolds number are assumed. Thus, the field equations are represented by

$$\text{div} j = 0 \tag{4}$$

$$\text{rot} E = 0 \tag{5}$$

In the calculations, the following assumptions are also made:

1) The temperature T_g and velocity u_r of the heavy particles are constant in the generator.
2) Only single ionization of atoms by electron-atom collisions and three-body recombinations are considered.
3) Magnetic field B is uniform in space.

Numerical calculations are carried out by transforming Eqs. (1-5) to a cylindrical (r, θ) coordinate system as outlined in Ref. 4.

The coordinate system and channel geometry in the calculation are shown in Fig. 1, where the generator size is the same as mentioned in Ref. 4 and a channel of constant cross section is assumed. The directions of the magnetic field and gas flow are also shown in this figure.

As the inlet boundary conditions, a constant electron temperature of 3500 K and a constant electron number density of one-half of the Saha equilibrium value at that temperature are assumed. To reduce calculation time, an inlet boundary electron temperature of 3500 K is assumed: this is not far from reality, because the plasma radiation can be observed close to the anode.[12] The outlet boundary condition is assumed to be $(\partial T_e/\partial r)_{out} = 0$. As the electrical boundary condition, the potential function ϕ is assumed to be zero at the anode. The initial and inlet electron temperatures are assumed to be the same and a Gaussian distributed disturbance with a standard deviation of 10 K is introduced. The initial electron number density is the Saha equilibrium value at the initial temperature.

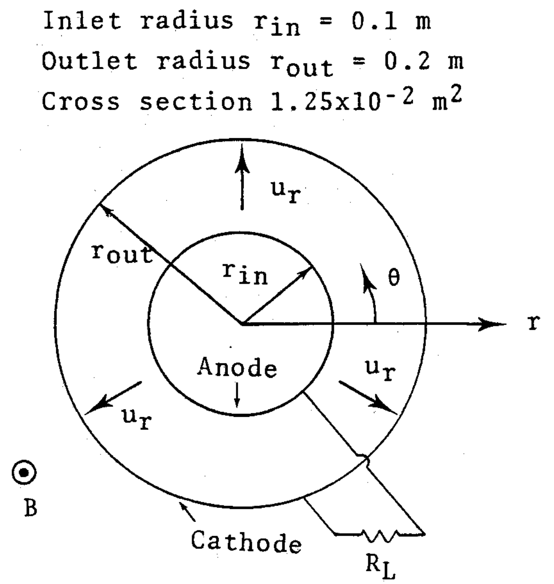

Fig. 1 Schematic view of the disk generator used in the numerical calculations.

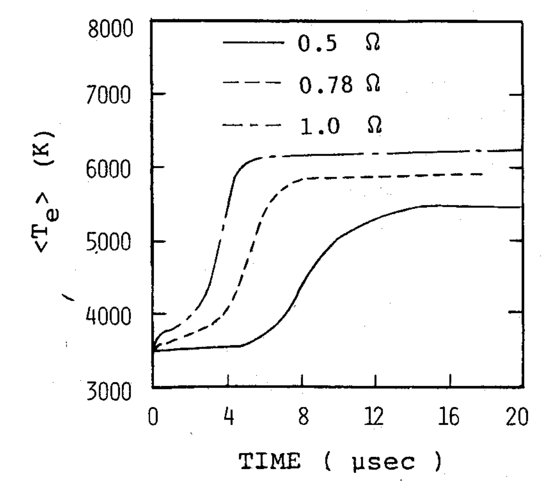

Fig. 2 Evolution of the averaged electron temperature $\langle T_e \rangle$ with time for three values of the load resistance at $B = 3.5$ T.

Simulations are based on the finite difference method, where the generator channel is divided into 20 mesh points in the r direction and 100 mesh points in the θ direction. Several cases of power generation are considered, the gasdynamic conditions, magnetic field strength, and load resistance of which are summarized in Table 1.

Results and Discussion

Ar/K Working Gas

For working gas Ar/K, the effect of the magnetic field and load resistance on the plasma is investigated in detail. Figure 2 shows the intital evolution of the electron temperature averaged over the generator channel for three values of the load resistance, where the averaged electron temperature is defined as

$$\langle T_e \rangle = \sum_i^N n_e(i) T_e(i) \Big/ \sum_i^N n_e(i) \tag{6}$$

where $T_e(i)$ and $n_e(i)$ are the electron temperature and electron number density at the ith mesh element of the generator, respectively, and N the total number of meshes. In this case, the time at which the plasma in the generator reaches steady state becomes shorter as the load resistance increases. The initial evolution time of the plasma also depends on the magnetic field, seed material, and gasdynamic constants. The high Joule heating conditions accelerate the growth of the plasma.

The plasma structures in the generator at the end of calculations are shown in Figs. 3 and 4, where distributions of the current stream function ψ and the θ directionally averaged electron temperature $\langle T_e \rangle_\theta$ are shown, respectively. The current stream function ψ is introduced by

$$j_r = \left(\frac{1}{rh}\right)\left(\frac{\partial \psi}{\partial \theta}\right), \quad j_\theta = \left(-\frac{1}{h}\right)\left(\frac{\partial \psi}{\partial r}\right) \tag{7}$$

using height h of the generator channel.

The steady state is certified by the stationary behavior of the averaged electron temperature and its variation around the mean value. It is found that the plasma is uniform and in a fully ionized state, except in the inlet region. The inlet region is occupied by plasma having a low electron temperature. From the direction of the current streamline, it is clear that the plasma in the inlet region does not generate electric power, but rather consumes the power generated in the downstream region. The values of total output current I_r is also included in Fig. 3. As the electron temperature increases in the fully ionized plasma, the θ component of the current increases and I_r slightly decreases. The effect of the Lorentz force may become stronger for plasma with a higher electron temperature, but the details are beyond the scope of this discussion. Within our simulation, the influence of $j_r B$ on the flowfield is much smaller and, therefore, the swirl flow of heavy particles can be neglected.

An important feature of steady-state plasma in the generator is shown in Fig. 5 where the magnetic field is decreased from 3.5 to 2.5 T. The current streamline distributions have nearly the same trends as those in the case of $B = 3.5$ T, at the time when the total output current becomes smaller because of the small induced electrical field. The θ directionally averaged electron temperatures are plotted along the r direction in Fig. 6. When the load resistance remains same, the width of the relaxation region becomes almost same for both of these magnetic fields, but the value of the electron temperature of the uniform plasma generating the power is lower for $B = 2.5$ T than for $B = 3.5$ T. As far as the plasma structure is concerned, it is found from Figs. 4 and 6 that the load resistance influences the width of the relaxation region and the magnetic field influences the growth rate of the plasma and electron temperature in the uniform region near the cathode, but both prominently affects the Joule heating of

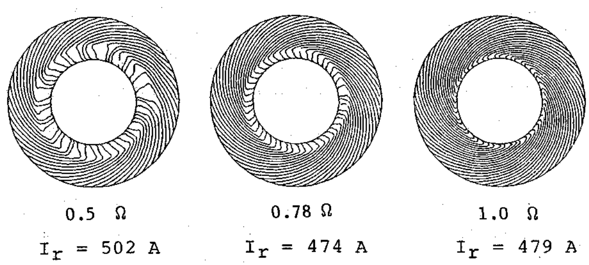

Fig. 3 Distribution of the current streamlines with an interval of 1/100 total current for several load resistances. Total current is shown by I_r.

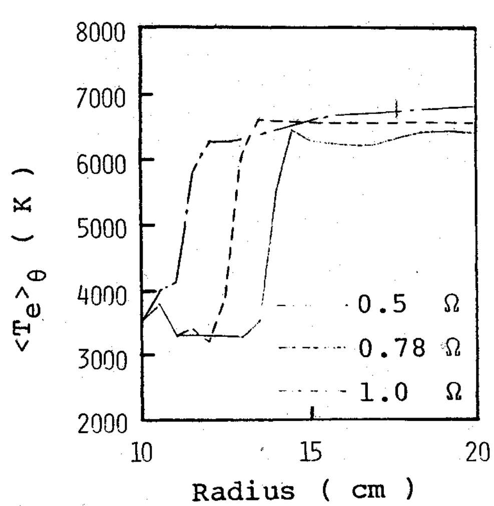

Fig. 4 Distributions of electron temperature averaged over the tangential direction of the channel for $B = 3.5$ T.

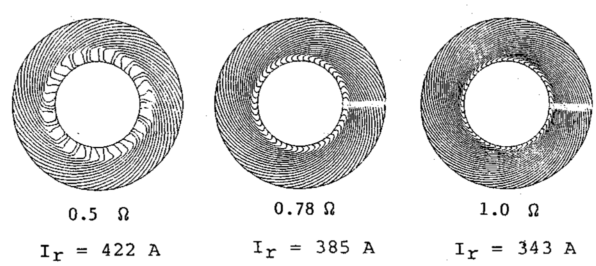

Fig. 5 Distributions of the current streamlines for $B = 2.5$ T.

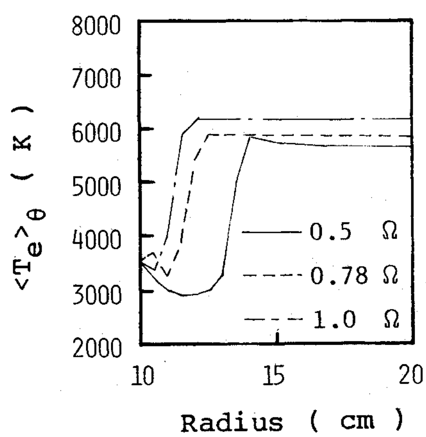

Fig. 6 Distributions of electron temperature averaged over the tangential direction of the channel for $B = 2.5$ T.

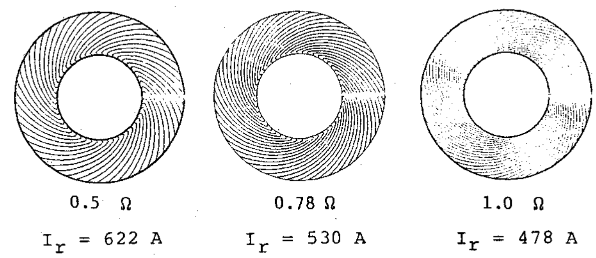

Fig. 7 Distributions of the current streamlines for the Ar/Cs plasma ($B = 3.5$).

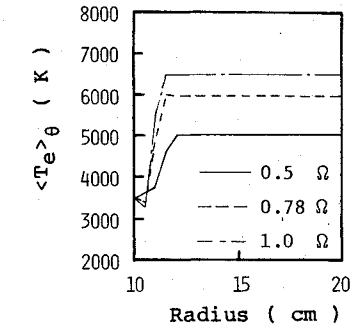

Fig. 8 Distributions of $\langle T_e \rangle_\theta$ along r direction of the channel for Ar/Cs plasma ($B = 3.5$ T).

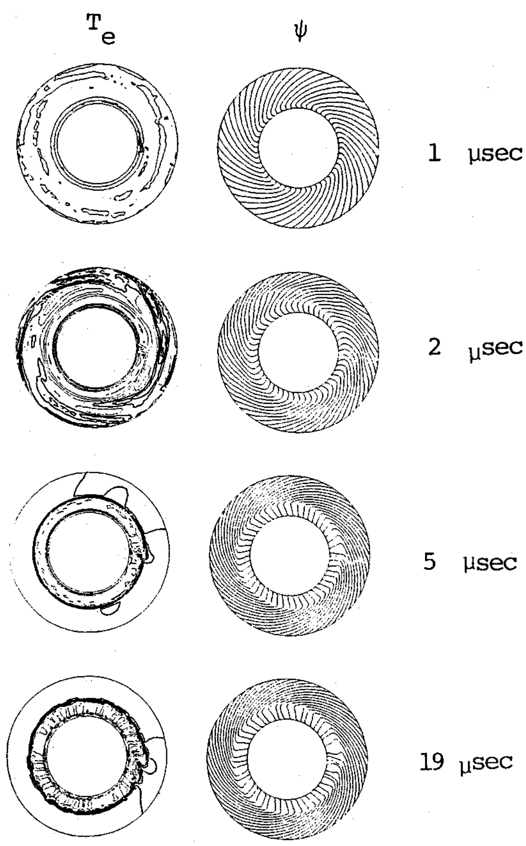

Fig. 9 Distributions of isothermal lines of T_e and current streamlines for four different time instances (the interval 500 K is used for the electron temperature). Conditions: He/K, $R_L = 0.6\ \Omega$, $B = 3.5$ T.

the plasma. The same results were obtained in r-z two-dimensional analyses.[13,14]

Now we would like to discuss the effect of electron temperature boundary condition on the growth of the plasma. For electron temperatures above 2800 K, we get the same results. For much lower values of electron temperatures (such as 2000 K), the plasma grows very slowly—and sometimes it does not develop within the limit of our computer calculation time. Here we assume the two-temperature model, so the behavior of the plasma at such low electron temperatures is beyond the scope of this investigation. But, practically, the magnetic fields existing in the nozzle region can elevate the electron temperature, resulting in an inlet electron temperature of about 3000 K.[15]

Ar/Cs Working Gas

When we use cesium instead of potassium as the seed material, the plasma in the disk generator grows faster because

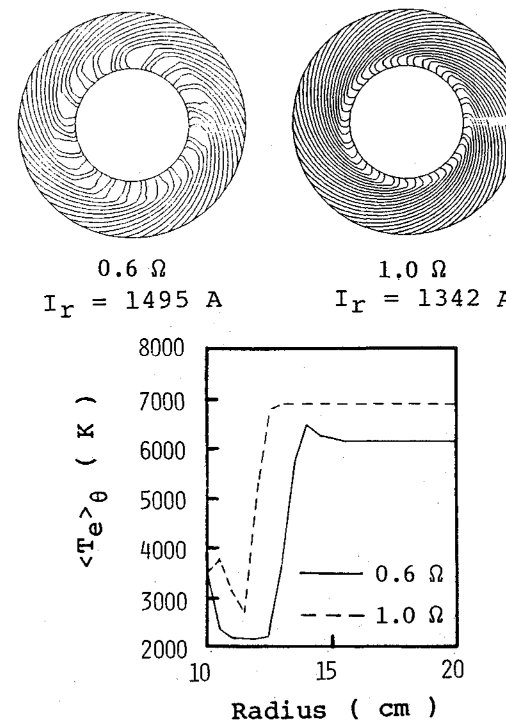

Fig. 10 Distribution of the current streamlines and $\langle T_e \rangle_\theta$ along r direction of the channel for conditions He/K, $B = 3.5$ T.

of cesium's low ionization potential. In Figs. 7 and 8, distributions of the current streamlines and $\langle T_e \rangle_\theta$ of a steady-state generator with cesium seed are described. A uniform plasma can be achieved in almost the entire generator. The properties of the plasma with Ar/Cs as the working gas indicate a better power generation performance than that with Ar/K. That is, the relaxation length of the plasma can be reduced; hence, more electrical current is produced when cesium is used as the seed material.

He/K Working Gas

In this section, it is investigated whether a steady-state plasma with a fully ionized seed can be dynamically realized with helium as the medium and how an almost three times higher gas velocity affects the width of the relaxation region. The gasdynamic conditions, magnetic field, and load resistance used for the simulations are listed in Table 1.

The stagnant gas pressure should be lower and the seed fraction higher with a working gas buffered by helium, than with one buffered by argon.[5] The lower stagnant gas pressure is needed to give a sufficient Hall parameter and the higher seed fraction is required to achieve the necessary conductivity.

Figure 9 shows the temporal developments in the isothermal lines of the electron temperature and current streamlines. It is seen that the plasma quickly reaches steady state at about 3 μs. The rapid growth in the plasma is induced by the higher gas velocity. Good uniform plasma is obtained throughout the generator, except in the relaxation region near the channel inlet. In Fig. 10, the distributions of the current streamlines and $\langle T_e \rangle_\theta$ are shown for the steady-state generator at two load resistances. From Fig. 10, it can be seen that the generator driven by seeded helium is filled with two states of plasma, as is the argon-driven generator. The inlet relaxation region can be reduced by suitably adjusting the load resistance. Since the gas velocity is high, a high power density is obtained in the same size generator, as happens when argon is the primary gas. From these plasma properties, it is inferred that the generator can be expected to perform efficiently when helium is used as an inert gas by suitably adjusting the gasdynamic conditions, magnetic field, and load resistance.

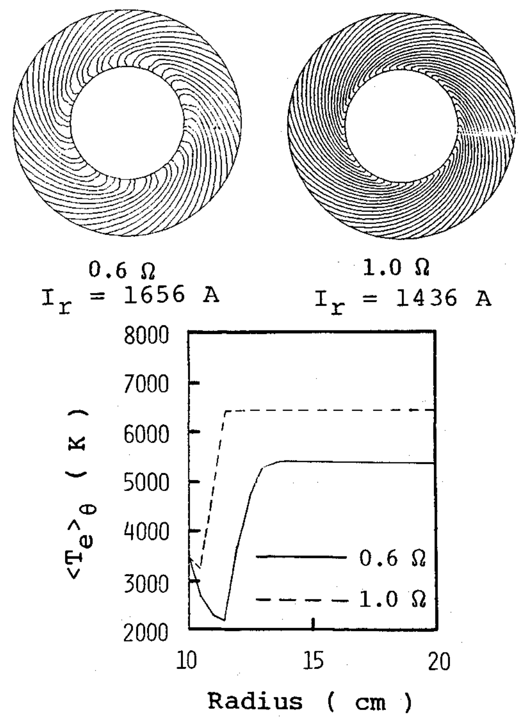

Fig. 11 Distribution of the current streamlines and $\langle T_e \rangle_\theta$ along r direction of the channel for conditions He/Cs, $B = 3.5$ T.

He/Cs Working Gas

Finally, helium seeded with cesium has been considered as the working gas. In this case, the growth of the plasma is the most rapid of the four working gases considered in this discussion. The distributions of the current streamlines and $\langle T_e \rangle_\theta$ along the r direction are shown in Fig. 11. As with argon, it is found that better uniformity and higher output currents are obtained with cesium as the seed material than with potassium.

Conclusions

The following results are obtained from r-θ two-dimensional, time-dependent numerical simulation:

1) In the four cases of MHD generator working gases under consideration, stable plasma with a fully ionized seed can be dynamically realized in a disk-type generator channel.

2) Using cesium as the seed material results in better performance because of its lower ionization potential as compared to potassium.

3) By replacing argon with helium as the inert gas, good generator performance can be achieved by suitably adjusting the gasdynamic conditions, magnetic field, and load resistance.

Acknowledgments

The authors gratefully acknowledge the support of Profs. S. Shioda and H. Yamasaki. The authors also wish to thank Mr. D. Biswas for his help with the English translation. Some part of this work was performed as a cooperative research project with the Plasma Laboratory of Nagoya University and was supported by a Grant-in-Aid for Energy Research from the Japanese Ministry of Education.

References

[1]Nakamura, T. and Riedmüller, W., "Stability of Nonequilibrium MHD Plasma in the Regime of Fully Ionized Seed," *AIAA Journal*, Vol. 12, 1974, pp. 661-668.

[2]Shioda, S. et al., "Power Generation Experiments and Prospects of Closed Cycle MHD with Fully Ionized Seed," *Proceedings of 7th International Conference on MHD*, Vol. 2, 1980, pp. 685-695.

[3]Abed, T., Kabashima, S., Yamasaki, H., and Shioda, S., "Theoretical Studies on Closed Cycle MHD Generator with Fully Ionized Seed," *Energy Conversion and Management*, Vol. 22, 1982, pp. 251-261.

[4]Yoshikawa, Y., Kabashima, S., Yamasaki, H., and Shioda, S., "Dynamic Properties of Nonequilibrium Plasma in Disk MHD Generator," *Journal of Propulsion and Power*, Vol. 1, 1985, pp. 425-431.

[5]Okuno, Y., Kabashima, S., Yamasaki, H., Harada, N., and Shioda, S., "Comparative Studies of the Performance of Closed Cycle Disk MHD Generators Using Argon, Helium, and Argon-Helium Mixture," *Energy Conversion and Management*, Vol. 25, 1985, pp. 345-353.

[6]Yamasaki, H. et al., "Closed Cycle MHD Disk Experiments at T.I.T.," *Proceedings of 23rd Symposium on Engineering Aspects of MHD*, 1985, pp. 430-438.

[7]Rosa, R.J., *Magnetohydrodynamic Energy Conversion*, MacGraw-Hill Book Co., New York, 1963, Chap. 5.

[8]Mitchner, M. and Kruger, C.H., *"Partially Ionized Gases*, John Wiley & Sons, New York, 1973, Chap. 5.

[9]Hara, T., Veefkind, A., and Rietjens, L H.Th., "Numerical Simulation of Inhomogeneous Discharge Structure in Noble Gas MHD Generator," *AIAA Journal*, Vol. 20, pp. 1473-1480.

[10]Hinnov, E. and Hirshberg, J.G., "Electron-Ion Recombination in Dense Plasma," *Physical Review*, Vol. 125, 1962, pp. 795-801.

[11]Hiramoto, T., "Rates of Total and Local Radiative Energy Losses in Nonequilibrium Plasma," *Journal of the Physical Society of Japan*, Vol. 26, 1969, pp. 785-801.

[12]Harada, N. et al., "Effect of Ionization Relaxation and Potential Drop near Electrode on Fully Ionized Seed Closed Cycle MHD Generator," *Proceedings of 8th International Conference on MHD*, 1983, pp. M13.1-M13.4.

[13]Fukuda, H. and Kabashima, S., "Ring-Shaped Discharge Structures in a Closed Cycle MHD Disk Generator," *Journal of Propulsion and Power*, to be published.

[14]Okuno, Y., Yamasaki, H., Kabashima, S., and Shioda, S., "Performance of Closed Cycle Disk Generator with High MHD Interaction," Paper presented at 8th Symposium on Efficient Use of Energy and Direct Electrical Power Generation, March, 1986 (in Japanese).

[15]Harada, N., Yamasaki, H., and Shioda, S., "Experiments in Shock-Tube Driven Closed Cycle MHD Generators with Seeded Helium," Paper presented at U.S./Japan Seminar on MHD Power Generation, March 1986.